

## Nuclear Magnetic Resonance in Single Crystals of CdS

TOSHIMOTO KUSHIDA AND A. H. SILVER

*Scientific Laboratory, Ford Motor Company, Dearborn, Michigan*

(Received 7 October 1964)

The  $\text{Cd}^{111}$  and the  $\text{Cd}^{113}$  NMR lines in CdS single crystals were studied at 4.2°K. The spin-lattice relaxation time  $T_1$  of high-resistivity samples is strongly affected by optical illumination. A typical value of  $T_1$  for a sample cooled in the dark,  $3 \times 10^8$  min, decreased to 30 min while the sample was being illuminated with white light. If the sample was kept at 4.2°K,  $T_1$  did not return to the original value but remained at about  $4 \times 10^2$  min after the light was turned off. Bleaching with red light restored  $T_1$  to  $1.4 \times 10^8$  min. The lifetime  $T_{1p}$  of the nuclear-spin polarization in the rotating frame was measured as a function of rf field strength  $H_1$  under various illumination conditions.  $T_{1p}$  decreases very rapidly when  $H_1$  is decreased below 1 G. Light-created trapped paramagnetic centers are mainly responsible for these relaxation effects. In order to fit the data with nuclear-spin diffusion theory, it was necessary to consider at least three different types of trapped centers. The density of these centers under various illumination conditions was estimated. NMR signals of nuclei near the trapped centers were observed using a double-resonance technique in the rotary frame. A strong signal of  $\text{S}^{33}$  was also found using this technique.

### I. INTRODUCTION

WHEN a photoconductor is illuminated, photoelectrons are created and some of these electrons may be trapped at lattice defects and/or impurities. The trapped electrons, if they are paramagnetic, decrease the nuclear spin relaxation time  $T_1$  through nuclear spin-diffusion processes.<sup>1</sup> The photoelectrons in a conduction band could also decrease  $T_1$  via hyperfine coupling<sup>2</sup> and could even shift the frequency of the NMR line as in the case of semiconductors,<sup>3</sup> if their density is large enough. While many results have been reported on paramagnetic relaxation of nuclei, the effect of optical illumination on NMR has not been reported.<sup>4</sup> We observed a large change (two orders of magnitude) in  $T_1$  of the  $\text{Cd}^{111}$  and  $\text{Cd}^{113}$  NMR lines when a photoconductive CdS crystal was illuminated with white light at liquid-He temperature.

Since the density of the photoelectrons is low in the present experimental condition compared with the light-created trapped centers, the observed change in  $T_1$  is predominantly caused by these centers. In order to analyze the spin-diffusion process, it is desirable to know the magnetic field dependence of  $T_1$  over a wide range of effective magnetic fields, particularly at low fields. It was found that the measurement of an effective spin-lattice relaxation time in a rotary frame  $T_{1p}$ <sup>5-13</sup> is

very useful. An effective magnetic field  $\mathbf{H}_{er}$ , seen in a coordinate system which is rotating at the angular frequency of an rf magnetic field  $H_1$ , is<sup>5</sup>

$$\mathbf{H}_{er} = [H_0 - (\omega/\gamma)]\mathbf{k}_r + H_1\mathbf{i}_r, \quad (1)$$

where  $\mathbf{i}_r$  and  $\mathbf{k}_r$  are unit vectors in the rotating coordinate system.  $T_{1p}$  can be measured as a function of  $H_{er}$  down to very low fields, while the laboratory field,  $H_0$  is kept high.

An important point, as far as the analysis of the spin-diffusion process is concerned, is that since the relaxing agents, electron spins, are still in the laboratory frame, the spectrum of these electron spins, which provide the necessary Fourier components to relax the nuclear spins, is unchanged. On the other hand, if we should attempt to measure  $T_1$  at low field in the laboratory frame, the electron spin spectrum would also be altered with the decrease of the field. The analysis of the spin diffusion then becomes more complex. Furthermore, the NMR resonance frequency may cross with another species of nucleus<sup>6</sup> and/or cross with other EPR lines of some impurities. In other words, we have maintained the heat sink constant while studying the field dependence of  $T_1$  in the rotating frame.

The rotary-frame experiment permits two different types of spins to sit in two different and independently controlled fields,  $H_{er}$  and  $H_0$  in the case mentioned here. The second field can be another effective field in another rotary frame rotating with the second spin. The feasibility of selecting two effective fields independently permits us to selectively cross relax almost any two types of spins.<sup>8</sup> It has been demonstrated that the cross relaxation can be used to detect very weak NMR signals in the laboratory frame.<sup>14,15</sup> The applicability of this laboratory-frame method is limited to cases of large quadrupole or hyperfine interactions or else requires reduction of the laboratory field near zero.

<sup>1</sup> N. Bloembergen, *Physica* **15**, 386 (1949).

<sup>2</sup> See for instance, A. Abragam, *The Principle of Nuclear Magnetism* (Oxford University Press, London, 1961), p. 390.

<sup>3</sup> I. Weinberg, *J. Chem. Phys.* **39**, 492 (1963).

<sup>4</sup> After the completion of this experiment, Professor W. Low mentioned that he also noticed a marked decrease of  $T_1$  in CdS when it was illuminated.

<sup>5</sup> A. G. Redfield, *Phys. Rev.* **98**, 1787 (1955).

<sup>6</sup> N. Bloembergen and P. P. Sorokin, *Phys. Rev.* **110**, 865 (1958).

<sup>7</sup> C. P. Slichter and W. C. Holton, *Phys. Rev.* **122**, 1701 (1961).

<sup>8</sup> S. R. Hartman and E. L. Hahn, *Phys. Rev.* **128**, 2042 (1962).

<sup>9</sup> F. M. Lurie and C. P. Slichter, *Phys. Rev. Letters* **10**, 403 (1963).

<sup>10</sup> A. G. Redfield, *Phys. Rev.* **130**, 589 (1963).

<sup>11</sup> F. M. Lurie and C. P. Slichter, *Phys. Rev.* **133**, A1108 (1964).

<sup>12</sup> D. Ailion and C. P. Slichter, *Phys. Rev. Letters* **12**, 169 (1964).

<sup>13</sup> R. E. Slusher and E. L. Hahn, *Phys. Rev. Letters* **12**, 246 (1964).

<sup>14</sup> A. A. Silvidi and J. W. McGroth, *J. Chem. Phys.* **33**, 1789 (1960).

<sup>15</sup> S. Nakamura and H. Enokiya, *J. Phys. Soc. Japan* **18**, 183 (1963).

Almost any two species of spins can be selectively cross-relaxed in the rotary frames because of the independent choices of the two  $H_{er}$ 's. The nuclear relaxation due to paramagnetic impurities can be considered as a crossing between the NMR line and zero-frequency EPR lines. The crossing in the rotary frames has been used very successfully in detecting very weak signals of minority species.<sup>8-10,13</sup> It has a remarkable sensitivity and applicability.

In this paper, observation of the  $S^{33}$  NMR line and the NMR lines of those Cd nuclei within a diffusion barrier region about the paramagnetic centers<sup>1</sup> in CdS are reported, using this double-resonance technique in the rotary frame.

## II. EXPERIMENTAL PROCEDURE

Single crystals of CdS were purchased from Eagle-Picher Company. Most of the experiments were carried out using Eagle-Picher Grade C high-purity CdS. According to the chemical analysis by the manufacturer, this sample contains ppm impurities as follows: Si, 4.0; Mg, 0.5; Fe, 0.5; Al, 0.5; Cu, 0.5; In, 30; Zn, 100; and Ca, 0.3. Similar results were obtained with Eagle-Picher Grade A and B samples, although an extensive study was not carried out with these samples. The dimension of the single crystal sample is about  $8 \times 8 \times 20$  mm.

A sample head is shown in Fig. 1. The CdS sample was placed in the inside rf coil  $L_1$  with the  $c$  axis of the crystal aligned along the external magnetic field  $H_0$ . The sample was illuminated through a quartz rod. An outer rf coil,  $L_2$ , with axis perpendicular to that of  $L_1$ , is for the double-resonance experiment. The total assembly was immersed in liquid He. The light from a 6 V light bulb was focused at the top of the quartz rod. The block diagram of the measuring system is shown in Fig. 2. Sample coil  $L_1$  was connected to a bridge spectrometer, when the steady-state NMR signal was observed. The spectrometer consists of an Anderson null  $T$  bridge,<sup>16</sup> a low-noise amplifier, and a homodyne detector. Since  $T_1$  of  $Cd^{111}$  and  $Cd^{113}$  is extremely long at He temperature and the linewidth is very narrow,  $H_1$  in the sample must be very small in order to avoid saturation of the signal.

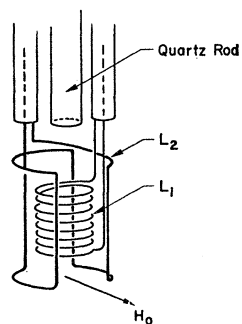


FIG. 1. The sample head. A CdS sample is placed in coil  $L_1$ . The outside coil  $L_2$  is for the double-resonance experiment. The sample is illuminated through the quartz rod.

The input rf voltage for the bridge spectrometer was less than 10 mV.

$T_1$  was measured using a saturation recovery method.<sup>1</sup> The signal was first completely saturated with a strong rf field, and the recovery of its intensity was measured using the bridge spectrometer. The signal intensity recovers exponentially.

Extremely long relaxation times for a "dark" sample were measured as follows: The saturation recovery was observed for about 100 min. The signal recovered only partially, and the recovery curve was almost a straight line. Then the sample was illuminated, and the saturation recovery was measured under illumination. Since the  $T_1$  value under illumination is about 30 min, more than 90% of the recovery curve  $I_0(1 - \exp[-t/T_1])$  can be observed in about 100 min. The value  $I_0$  thus obtained and the initial slope of the former slow recovery curve for the dark sample make the measurement of the long  $T_1$  possible, if  $I_0$  for the two cases is the same. Spectrometer sensitivity was stable enough to make a reliable intensity measurement. If the optical illumination were to produce a nuclear polarization through photoelectrons, the value of  $I_0$  under illumination would be different from the value when the sample is kept dark. This possibility, which would be very interesting if it existed, was excluded for the present illuminating condition as follows: First, the intensity of the signal was fully developed by spending enough time under illumination. Then the light was turned off, and the intensity of the signal was measured after several hours. If the light had produced the nuclear polarization, the signal intensity should have decreased after a fraction of  $T_1$ . However, no intensity change was observed.

$T_{1p}$  was measured using an rf oscillator  $Osc_1$  and an amplifier  $Amp_1$  as follows: The magnetic field was first

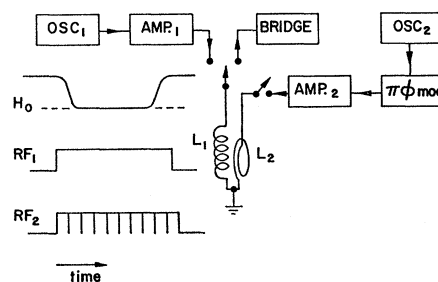


FIG. 2. The block diagram of the measuring system. The ordinary NMR signal was observed using an Anderson bridge.  $Osc_1$  and  $Osc_2$  are Hewlett-Packard 606A oscillators.  $Amp_1$  is a Boonton Power Amplifier 230A, and  $Amp_2$  is a three IFI Wide-band Amplifier 500A's in series. A strong rf field in  $L_1$  produced by  $Osc_1$  and  $Amp_1$  was used to bring a first spin system into the rotary frame in conjunction with an adiabatic magnetic field change. In the case of a double-resonance experiment in the rotary frame, a second species of nucleus was brought into the rotary frame using  $Osc_2$  and  $Amp_2$  simultaneously with the first spin system. The phase of the second rf was periodically flipped by  $180^\circ$  ( $\pi\phi$  mod). The sequence of the static field change, the first rf field, and the second  $\pi\phi$  modulated rf field is shown at the lower left side.

<sup>16</sup> H. L. Anderson, Phys. Rev. **76**, 141 (1949).

shifted to an off-resonance value, and the sample coil was switched to  $\text{Osc}_1$  and  $\text{Amp}_1$ .  $\text{Osc}_1$  is a Hewlett Packard 606 rf oscillator and  $\text{Amp}_1$  is a Boonton rf amplifier, which produces an rf voltage up to 30 V across  $L_1$ . The magnetic field was adiabatically brought to the resonance value. The adiabatic condition here is<sup>7</sup>

$$(1/H_{er})(dH_{er}/dt) \ll (\gamma H_{er}/2\pi), \quad (2)$$

where

$$H_{er} = [(H_0 - \omega/\gamma)^2 + H_1^2]^{1/2}. \quad (3)$$

Since  $dH_{er}/dt$  was about 10 G/sec and the minimum value for  $\gamma H_{er}/2\pi$  was about 700 cps ( $\gamma H_1/2\pi$ ), the adiabatic condition was well satisfied. The spin-lattice relaxation during this process was negligible. The nuclear spin magnetic moment was thus brought into the rotating frame;<sup>7</sup> that is, the total spin moment  $M_z$  was tipped in the direction of the effective field  $\mathbf{H}_{er} = \mathbf{H}_1$ . The spins which had originally aligned along the static magnetic field of the order of 10 000 G were thus adiabatically demagnetized to  $H_1$ . The spin temperature is initially very low in this demagnetized state, and it tends to return to the lattice temperature in  $T_{1p}$  by shrinking the magnetic moment along  $H_1$ . After spending a certain time in the rotating frame, the magnetic field was adiabatically brought back to the off-resonance value. The remaining total spin moment was thus brought back to the direction of  $H_0$ . The rf field  $H_1$  was reduced to a very low level,  $L_1$  was switched to the spectrometer, and the steady-state NMR signal was observed by sweeping the magnetic field. The intensity ratio between the signal thus measured and the original signal before entering the rotating frame decreases exponentially with the time spent in the rotary frame. The time constant gives  $T_{1p}$  for the particular value of  $H_1$  in which the spins were demagnetized. The magnetic field was modulated at 35 cps, when the steady-state signal was observed. The modulation was turned off when the spin system was brought into the rotary frame in order to avoid a loss of the spin polarization due to a rotary saturation effect.<sup>5</sup> Although the present modulation frequency is much lower than the minimum Larmor frequency in the rotary frame, 700 cps, the harmonics of the modulation signal might produce rotary saturation. The magnitude of  $H_1$  was calibrated using the rotary saturation phenomenon.<sup>5</sup>

The second minority nucleus was detected using Hahn's double-resonance technique in the rotary frame.<sup>8</sup> The minority nucleus was brought into the rotary frame simultaneously by sending a second strong rf field to  $L_2$ . The second rf was provided using another Hewlett Packard 606 oscillator and three IFI wide-band amplifiers in series, and the frequency was adjusted to the Larmor frequency of the second nucleus in the laboratory field. The Larmor frequencies for the two different nuclei in their rotating frames can then be matched by adjusting the relative magnitude of the two

rf magnetic fields so that

$$\gamma_1 H_{11} = \gamma_2 H_{12}. \quad (4)$$

Here,  $H_{11}$  and  $H_{12}$  are  $H_1$  for the first and the second rf, respectively.  $\gamma_1$  and  $\gamma_2$  are  $\gamma$  values for the two nuclei. The condition (4) enables the two different nuclei to make a maximum thermal contact in the rotary frame. The matching of the Larmor frequencies in the rotary frame can also be achieved between the same kind of nuclei in different local fields.<sup>13</sup>

When both nuclei are brought into the rotary frame, the phase of the second rf field  $H_{12}$  is nonadiabatically flipped  $\pi$  radians. The phase must be switched faster than the Larmor period for  $H_{er}$ , i.e., faster than  $2\pi/\gamma H_{12} \simeq 10$  msec. Then the temperature of the second spin system in its rotating frame becomes negative, and the energy starts to flow from the second to the first spin system. If the spin specific heat of the second system is much smaller than the first system, which is usually the case when the second species is in the minority, this single process is not sufficient to warm up the first system appreciably. The cooled-down second system can, however, be brought to a negative temperature again and again by repeating the  $\pi$  phase switching process. Thus a very weak NMR signal from the second system can be observed as a loss of the spin magnetization of the first (majority) system in the rotary frame.

Since  $T_1$  of the sample is sufficiently long, all the manipulations were done manually, although automatic switching can be done without much trouble.

### III. EXPERIMENTAL RESULTS AND INTERPRETATION

The NMR line shapes for  $\text{Cd}^{111}$  and  $\text{Cd}^{113}$  are Gaussian, and the linewidth as measured from the maximum to the minimum slope of its derivative curve is  $282 \pm 17$  cps for  $\text{Cd}^{113}$ . Optical illumination caused no frequency shift within the experimental error of  $2 \times 10^{-6}$ .

#### A. $T_1$ and $T_{1p}$

Figure 3 shows the longitudinal relaxation time of the  $\text{Cd}^{113}$  NMR for the single crystal of CdS Grade C both in the laboratory ( $T_1$ ) and the rotary ( $T_{1p}$ ) frames under various illumination conditions. The range of the measured relaxation times was from 20 sec to 300 min. Measured values of  $T_1$  are shown at the right side of the figure. When the sample was cooled to He temperature in the dark,  $T_1$  was about 3000 min. The dc resistivity is larger than 100 M $\Omega$  cm, [points (a)].

While the sample was being illuminated with white light,  $T_1$  reduced to about 30 min [curve (d)]. The resistivity decreased gradually when the light was turned on. It required several minutes to reach the final value, about 1 M $\Omega$  cm.

When the light was turned off, the  $T_1$  value recovered only to about 400 min [curve (c)].  $T_1$  was observed to remain at this value for more than 10 h (it probably

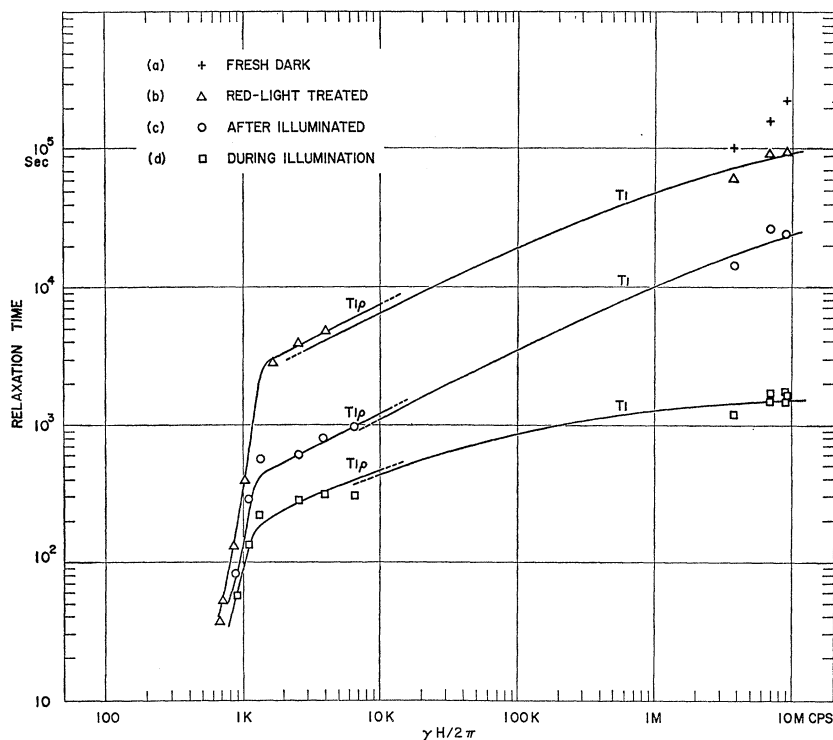


FIG. 3.  $T_1$  and  $T_{1\rho}$  of  $\text{Cd}^{113}$  under various illuminating conditions. The longitudinal relaxation time is plotted as a function of  $\gamma H/2\pi$  both in the laboratory frame ( $T_1$ ) and in the rotary frame ( $T_{1\rho}$ ).  $T_1$  for (a) fresh dark sample, (d) during illumination with white light, (c) after illumination with white light, and (b) red-light treated sample after illumination with white light, is shown at the right side.  $T_{1\rho}$  for the conditions (b), (c), and (d) is shown at the right side. The curves represent Eqs. (22) and (23) with the values of parameters shown in Table I.

persists indefinitely) as long as the sample was kept in the dark at He temperature. The resistivity, however, increased by only several percent when the white light was turned off. Most of the conductance once created by the light persists after the light is turned off.

If the sample is treated with red light,  $T_1$  returns almost to the value for the fresh dark sample [curve (b)]. The red light was provided by inserting a red filter, Corning 7-57, at the top end of the quartz rod. This filter cuts off the light whose wavelength is shorter than about 8000 Å.

The  $T_1$  values were measured at three different values of the static magnetic field, 9700, 7400, and 4030 G.  $T_1$  tends to decrease with a decrease of the magnetic fields. This is in agreement with the idea that the nuclear relaxation is predominantly caused by nuclear spin diffusion<sup>1,17</sup> toward the paramagnetic centers.

The relaxation time in the rotary frame  $T_{1\rho}$  is shown by the experimental points at the left side of Fig. 3. It decreases very sharply below  $\gamma H_{er} = \gamma H_1 \approx 1$  kc/sec.  $T_{1\rho}$  changes as fast as  $(\gamma H_1)^6$ . This sharp decrease takes place at a much higher field than the local dipole field of the Cd nucleus, which is of the order of 0.15 G.

As demonstrated by Slitcher and Holton,<sup>7</sup> if there is no irreversible process which couples with the spin system,  $T_{1\rho}$  is essentially as long as  $T_1$  even in the case of  $H_1 \approx 0$ . When the effective field  $H_{er}$  in Eq. (3) is reduced adiabatically below the local field, the spin-magnetic moment along  $H_{er}$  decreases reversibly; that

is, the magnetic moment can be recovered reversibly by increasing  $H_{er}$  adiabatically, if the whole process is done within  $T_1$ . If the spin system is coupled *directly* with a second spin system with a much shorter relaxation time, Bloembergen and Sorokin<sup>6</sup> showed that  $T_{1\rho}$  decreases as  $(\gamma H_1)^2$  with decreasing values of  $H_1$ . Therefore, the decrease of  $T_{1\rho}$  observed in the present case is much steeper than any previously reported.

The large decrease in  $T_1$  and  $T_{1\rho}$  by the optical illumination may be attributed to (i) conduction electrons created by the illumination and (ii) an increase of the paramagnetic centers. In the present case, the effect of the conduction electrons on the nuclear relaxation is masked by the much larger effect due to the paramagnetic centers. The density of photoconduction electrons is estimated as the order of  $10^{11}$ /cc during the illumination, assuming the mobility of the electrons is 100 cm/V. This value is much smaller than the density of the paramagnetic centers. The paramagnetic centers result from the trapping of photoelectrons at defect sites. Most of the trapped electrons will relax nuclear spins via spin diffusion processes. The trapped photoelectrons are continuously accumulated at the defects, and their density becomes of the order of  $10^{16}$ , as will be shown later. The sluggish resistivity change when the light is turned on may be attributed to this accumulation process.

When the white light is turned off, some of the trapped electrons are released from the centers and return to the valence band, but the others remain

<sup>17</sup> A. Abragam, Ref. 2, p. 379 f.

trapped as long as the sample is kept in the dark and at low temperature. The change in  $T_1$  following white light illumination is due to these semipermanently trapped electrons [compare curves (d) and (c) in Fig. 3]. When the sample is treated with red light, most of these remanent centers are released and the nuclear relaxation time returns almost to the fresh dark values (a). Illumination of CdS with white light creates EPR lines which have been attributed to trapping centers, and illumination with red light destroys these EPR lines.<sup>18</sup>

No angular dependence of  $T_1$  or  $T_{1\rho}$  was observed within experimental error, when the angle between the  $c$  axis of the crystal and the magnetic field was altered.

The field dependence of  $T_1$  and  $T_{1\rho}$  will be interpreted using the spin-diffusion model which has been proposed by Bloembergen.<sup>1</sup> The transition probability of a nucleus coupled with a paramagnetic impurity is<sup>1</sup>

$$P = (3/4)(\gamma\gamma_e\hbar)^2 S(S+1)r^{-6} \sin^2\theta \cos^2\theta g(\nu). \quad (5)$$

Here  $r$  is the distance between the paramagnetic impurity and the nucleus,  $\theta$  is the angle which the line joining the nucleus and the impurity makes with the magnetic field, and  $\gamma_e$  is the gyromagnetic ratio of the paramagnetic electron. Bloembergen used a Debye function as the frequency distribution function  $g(\nu)$ :

$$g(\nu) = 2\tau/[1 + (2\pi\nu)^2\tau^2], \quad (6)$$

where  $\tau$  is a correlation time of the component of the electron spin  $S$ , and  $\nu$  is the nuclear Larmor frequency. Bloembergen considered the energy-flow process among the same species of nuclei through a nuclear spin flip-flop process. He derived an approximate relation for the probability of this process as

$$D \simeq (a^2/50T_2), \quad (7)$$

where  $T_2$  is nuclear spin-spin relaxation time, and  $a$  is the distance between the nuclei. Since  $1/T_2$  in Eq. (7) is the spin-flip probability among like nuclei, if  $T_2$  values are derived from the linewidth and include a contribution from other unlike nuclei, a correction must be made. Taking the average over angle in Eq. (5), the equation for the local population difference  $p$  between the nuclei with spin up and spin down was derived as

$$\partial p/\partial t = D\nabla^2 p - C(p - p_0)\sum_n (\mathbf{r} - \mathbf{r}_n)^{-6}, \quad (8)$$

where

$$C = 2\langle P \rangle_{\text{av}} = \frac{1}{5}(\gamma\gamma_e\hbar)^2 S(S+1)g(\nu), \quad (9)$$

and  $p_0$  is the thermal equilibrium value of  $p$ .

This diffusion equation was solved by Khutsishvili<sup>19</sup> and deGennes,<sup>20</sup> and discussed by Blumberg<sup>21</sup> for various conditions.  $T_1$ , due to this spin-diffusion process, was

derived as<sup>19,20</sup>

$$1/T_1 = 8.5NC^{1/4}D^{3/4}. \quad (10)$$

Here,  $N$  is the density of the paramagnetic centers. The criterion of the validity of Eq. (10) is

$$a, b < \rho < R, \quad (11)$$

where  $R$  is the average distance between the paramagnetic electrons,  $\rho$  is a pseudopotential radius

$$\rho = 0.68(C/D)^{1/4}, \quad (12)$$

and  $b$  is a critical radius, namely, within a sphere of radius  $b$  about the paramagnetic center, the local magnetic field produced by the center is larger than the nuclear dipole field. Therefore the diffusion process is inhibited within a radius  $b$  given by

$$b = (\mu_e/\mu)^{1/3}a, \quad \tau \gg [\gamma\langle H_S(r) \rangle_{\text{av}}]^{-1}, \quad (13a)$$

$$b = (\mu_e^2 H_0/\mu 3kT)^{1/3}a, \quad \tau \ll [\gamma\langle H_S(r) \rangle_{\text{av}}]^{-1}. \quad (13b)$$

Here,  $\langle H_S(r) \rangle_{\text{av}}$  is a proper average value of the local field produced by the paramagnetic electron. When  $\tau$  is infinite, the electron spin produces a static local field  $H_S(r) \simeq \pm\mu_e/r^3$ , where  $r$  is the distance from the electron. When  $\tau$  becomes finite,  $H_S$  fluctuates between  $\simeq +\mu_e/r^3$  and  $-\mu_e/r^3$ . If this fluctuation period  $\tau$  becomes shorter than the inverse of the local field, expressed as a nuclear frequency  $\gamma H_S$ , a typical motional narrowing takes place, and the nuclear spins see only the statistical average of the local field  $\simeq \mu_e(H_0\mu_e/3kT)$ . The collapsing of the diffusion barrier begins when  $\tau < T_2$ , since the value of  $b$  is determined by the condition that  $H_S(b)$  is equal to the nuclear dipole field. The diffusion barrier will be completely collapsed when  $\tau$  becomes short enough to average out the largest value of  $H_S(r)$  seen by the nucleus. The condition (11) was valid for the whole range of  $\nu$ ,  $\tau$ , and  $N$  for the present experiment.

According to Eqs. (6) and (9), the field and frequency dependence of  $T_1$  is

$$T_1 \propto H^{1/2} \propto \nu^{1/2}, \quad 2\pi\tau\nu \gg 1,$$

$$T_1 \propto H^0 \propto \nu^0, \quad 2\pi\tau\nu \ll 1.$$

Therefore, the slope of the  $\ln T_1$  versus  $\ln \nu$  is  $\leq \frac{1}{2}$ . If the relaxation is caused by more than one species of paramagnetic centers,

$$1/T_1 = \sum_i 1/T_1^{(i)} = 8.5 \sum_i N_i C_i^{1/4} D^{3/4}, \quad (14)$$

where  $N_i$  is the density of the  $i$ th type of paramagnetic centers and  $C_i$  is

$$C_i = \frac{2}{5}(\gamma\gamma_e\hbar)^2 S_i(S_i+1)\tau_i/(1 + (2\pi)^2\tau_i^2\nu^2). \quad (15)$$

Here again

$$0 \leq d \ln T_1 / d \ln \nu \leq \frac{1}{2}. \quad (16)$$

Although  $T_1$  has the same order of magnitude as  $T_{1\rho}$ ,  $T_1$  is not generally equal to  $T_{1\rho}$ <sup>5,22</sup> because of the follow-

<sup>18</sup> J. Lambe, J. Baker, and C. Kikuchi, Phys. Rev. Letters **3**, 270 (1959).

<sup>19</sup> G. R. Khutsishvili, Zh. Eksperim. i Teor. Fiz. **31**, 424 (1956) [English transl.: Soviet Phys.—JETP **4**, 382 (1957)].

<sup>20</sup> P.-G. deGennes, J. Phys. Chem. Solids **7**, 345 (1958).

<sup>21</sup> W. E. Blumberg, Phys. Rev. **119**, 79 (1960).

<sup>22</sup> I. Solomon and J. Ezraatty, Phys. Rev. **127**, 78 (1962).

ing reasons: (i) Matrix elements responsible for the nuclear relaxation are not equal in the two cases, and (ii) the effect of nuclear spin-spin interaction on the longitudinal relaxation time is not negligible at low effective field.

When the Zeeman field is equal to or smaller than the local field produced by the neighboring nuclei, the energy stored in the local field becomes comparable to or greater than that stored in the Zeeman field. Since the local-field part of the Hamiltonian  $H_d$  is quadratic with respect to the nuclear spin operator,  $H_d$  is expected to decay approximately twice as fast as the Zeeman part  $H_z$ , which is linear with respect to the spin operator. Therefore, the total spin Hamiltonian  $H_z + H_d$  decays somewhat faster than the individual spins do, and the decay time depends on the relative magnitude of  $H_z$  and  $H_d$ . It is this decay time of the total spin Hamiltonian that determines the decay time of spin temperature, which governs the thermal average value of  $H_z$  and  $H_d$ . This is also the decay time of the observed thermal average of the spin magnetization  $\langle M \rangle$  due to the relation

$$\langle M \rangle = -\langle H_z \rangle / H.$$

Thus Redfield<sup>5</sup> calculated the relation between the high-field and low-field relaxation times,  $T_1$  and  $T_{1l}$ , as

$$T_{1l} = T_1 \frac{1 + (\delta H)^2 / H_{er}^2}{1 + \alpha (\delta H)^2 / H_{er}^2}, \quad (17)$$

where  $\alpha$  is a numerical factor  $\approx 1.3-2$ , and the local field  $\delta H$  is defined as<sup>9,23</sup>

$$\delta H^2 = \frac{1}{3} \langle \Delta H^2 \rangle_{II} + \langle \Delta H^2 \rangle_{I'I'} \\ + \frac{1}{3} \frac{f_I \gamma_I^2 I'(I'+1)}{f_I \gamma_I^2 I(I+1)} \langle \Delta H^2 \rangle_{I'I'}. \quad (18)$$

Here  $\langle \Delta H^2 \rangle_{II}$  (or  $\langle \Delta H^2 \rangle_{I'I'}$ ) is the contribution of the  $I$  (or  $I'$ ) nuclear spins to their own second moment,  $\langle \Delta H^2 \rangle_{I'I'}$  is the contribution of  $I'$  spins to the  $I$  spin second moment, and  $f_I$  and  $f_{I'}$  are the fraction of  $I$  and  $I'$  spins. For Cd<sup>113</sup> in CdS,  $(\gamma/2\pi)\delta H \approx 120$  cps. Solomon and Ezratty have extended a similar calculation to the case of insulators with paramagnetic impurities,<sup>22</sup> whereas Redfield has considered the case of metals.

This correction is only important when  $(\delta H/H_1)^2 \geq 1$ . Therefore it is negligible for the present case, since  $(\delta H/H_{1 \min})^2 \approx 10^{-2}$ .

Now let us consider the differences in the spin-lattice relaxation matrix between the laboratory and the rotating frame. The transition probability in the laboratory frame, Eq. (5), was derived from Bloembergen's  $C$  and  $D$  term,<sup>1</sup>

$$-\frac{3}{2} \gamma \gamma_e \hbar^2 r^{-3} S_z(t) I_{\pm} \sin \theta \cos \theta e^{\mp i\Phi} e^{i\omega_0 t}.$$

The  $z$  component of the electron spin magnetic moment  $\hbar \gamma_e S_z$  fluctuates with a lifetime  $\tau$  and it generates an effective oscillating magnetic field in the  $xy$  plane which relaxes  $I_z$  at a rate proportional to the Fourier component of  $S_z^2$  at the nuclear Larmor frequency.

In the rotating frame the nuclear spin is quantized along  $H_{er}$ . The excess nuclear spin polarization along  $H_{er}$  is destroyed to its equilibrium value by an oscillating magnetic field in the plane perpendicular to  $H_{er}$  in the rotating frame, if the oscillating field satisfies a Larmor condition in the rotating frame,  $\gamma H_1 = \omega_r$  where  $\omega_r$  is the Larmor frequency in the rotary frame. The  $z$  component of such an oscillating field comes from Bloembergen's  $A$  term,

$$\gamma \gamma_e \hbar^2 r^{-3} S_z(t) I_z (1 - 3 \cos^2 \theta),$$

and only the Fourier component of  $S_z^2$  at  $\omega_r$  is effective for relaxation. The relaxing field perpendicular to the  $z$  axis comes from Bloembergen's  $C$  and  $D$  term with a Fourier component at  $\omega_r$  in the rotating frame. This frequency corresponds to  $\omega_0 \pm \omega_r \approx \omega_0$  in the laboratory frame. The relaxation rate in the rotating frame,  $C_r$  is calculated in the Appendix as

$$C_r = \frac{1}{5} S(S+1) \\ \times \hbar^2 \gamma^2 \gamma_e^2 \left( \frac{4}{3} \tau / (1 + \omega_r^2 \tau^2) + \tau / (1 + \omega_0^2 \tau^2) \right). \quad (19)$$

The first term is derived from the  $z$  component of the relaxing field and represents an effective field dependence of  $T_{1\rho}$ . The second term comes from the relaxing field perpendicular to the  $z$  axis and  $H_{er}$  and represents an  $H_0$  dependence of  $T_{1\rho}$ . Since  $\omega_0 \gg \omega_r$ , a similar relation to Eq. (16) holds for the dependence of  $T_{1\rho}$  on  $\omega_r (= 2\pi\nu_r)$ .

$$0 \leq d \ln T_{1\rho} / d \ln \nu_r < \frac{1}{2}. \quad (20)$$

The experimental results indicate that the relation (16) is well satisfied for 2 kc/sec  $< \nu < 10$  Mc/sec. The steep slope for  $\nu < 1.5$  kc/sec cannot, however, be explained by using the Debye function (6).

The increased slope for  $\nu < 1.5$  kc/sec suggests the presence of a much steeper shape function than Eq. (6). Pershan<sup>24</sup> observed a similar strong field dependence of the cross relaxation time  $T_{12}$  in LiF. We assume, therefore, that some species of paramagnetic centers have a Gaussian shape function

$$g(\nu) = 2(\sqrt{\pi}) \tau e^{-(2\pi\nu\tau)^2}. \quad (21)$$

At sufficiently low temperature such that the spin-lattice relaxation time of the electron spin  $T_{1e}$  is larger than an electron spin-spin relaxation time  $T_{2e}$ , the line shape of a zero-frequency EPR line could be expressed by Eq. (21) if the exchange narrowing is negligible. This line shape is, roughly speaking, an average packet line shape of the high-frequency EPR lines.

When  $T_{1e}$  is very long,  $g(\nu)$  in Eq. (6) does not have a sufficiently large amplitude at the nuclear Larmor fre-

<sup>23</sup> L. C. Hebel, Jr., *Solid State Physics* (Academic Press Inc., New York, 1963), Vol. 15, p. 456.

<sup>24</sup> P. S. Pershan, *Phys. Rev.* **117**, 109 (1960).

quency to relax the nucleus, since  $\tau = T_{1e}$ . The nuclei near an individual electron spin  $S_i$ , however, see predominantly the local-field fluctuation produced by the individual  $S_{zi}$  rather than the total spin  $\sum_i S_{zi}$ , whose lifetime is  $T_{1e}$ . Therefore the nuclei see the fluctuation of the local field with a characteristic period  $T_{2e}$ , which can be much shorter than  $T_{1e}$ . This  $T_{2e}$  process is temperature-independent. The nuclear energy is then transferred to this spin-spin bath first, and then released to the lattice through the  $T_{1e}$  process. The possibility of this spin-spin bath has been predicted by Bloembergen.<sup>1</sup> Experimentally, the presence of this bath has been proved recently<sup>25</sup> by directly heating this bath with a longitudinal audio-frequency magnetic field. The heating of the bath was observed by the temperature change of the surrounding nuclear spins in a single crystal of ruby (0.1% Cr in  $Al_2O_3$ ). This is the inverse of the nuclear relaxation via spin diffusion.

We propose that three types of trapped paramagnetic centers exist:

(i) Type 1, which has a Debye shape function, and the lifetime average over this group  $\tau$  is

$$\tau \simeq T_{1e} \simeq T_{2e} < 1/2\pi\nu.$$

(ii) Type 2, which also has a Debye shape function, but their average lifetime  $\tau'$  is

$$1/2\pi\nu < \tau' \simeq T_{1e}' \simeq T_{2e}' \lesssim 10^{-3}.$$

(iii) Type 3, which has a Gaussian shape function with the lifetime  $\tau''$

$$\tau'' \simeq T_{2e}'' \simeq 10^{-3} \leq T_{1e}''.$$

Now the experimental curves can be fitted by the following equations:

$$\frac{1}{T_1} = \frac{1}{T_1^{(0)}} \left[ n \left\{ \frac{2\tau}{1 + (2\pi\nu\tau)^2} \right\}^{1/4} + n' \left\{ \frac{2\tau'}{1 + (2\pi\nu\tau')^2} \right\}^{1/4} + n'' \left\{ 2\sqrt{\pi\tau''} e^{-(2\pi\tau''\nu)^2} \right\}^{1/4} \right], \quad (22)$$

and

$$\frac{1}{T_{1p}} = \frac{1}{T_1^{(0)}} \left[ n \left\{ \frac{2}{3} \frac{2\tau}{1 + (2\pi\nu\tau)^2} + \frac{1}{2} \frac{2\tau}{1 + (2\pi\nu\tau)^2} \right\}^{1/4} + n' \left\{ \frac{2}{3} \frac{2\tau'}{1 + (2\pi\nu\tau')^2} + \frac{1}{2} \frac{2\tau'}{1 + (2\pi\nu\tau')^2} \right\}^{1/4} + n'' \left\{ \frac{2}{3} \times 2\sqrt{\pi\tau''} e^{-(2\pi\tau''\nu)^2} + \frac{1}{2} \times 2\sqrt{\pi\tau''} e^{-(2\pi\tau''\nu)^2} \right\}^{1/4} \right]. \quad (23)$$

In Eq. (22) the second term gives the slope  $d(\ln T_1)/d(\ln \nu) = \frac{1}{2}$ , and the mixing of the first term decreases the slope to fit the experimental curve for a

<sup>25</sup> T. Kushida and A. H. Silver (to be published).

TABLE I. The parameters  $n$ ,  $n'$ , and  $n''$  in Eq. (18).

|                  | $n$ | $n'$ | $n''$           |
|------------------|-----|------|-----------------|
| (b) <sup>a</sup> | 1   | 17   | $8 \times 10^3$ |
| (c) <sup>b</sup> | 2   | 100  | 12              |
| (d) <sup>c</sup> | 90  | 200  | 15              |

<sup>a</sup> Red-light treated.  
<sup>b</sup> After illumination.  
<sup>c</sup> During illumination  
 $T_1^{(0)} = 6.0 \times 10^3$ .

relatively high value of  $\nu$ . The third term would give a steep slope when  $\nu \lesssim 1$  kc/sec, if  $T_1$  could be measured at such a low field without changing the electron heat-sink spectrum. The first bracket in Eq. (23) represents an essentially frequency-independent term. The second bracket gives a slope  $d(\ln T_{1p})/d(\ln \nu_r) \approx \frac{1}{2}$ , since the second term in the bracket is much smaller than the first. In the third bracket the second term is negligible compared with the first term which gives the steep slope when  $\nu_r \lesssim 1$  kc/sec. The lifetime  $\tau$  and  $\tau'$  were chosen rather arbitrarily as

$$\tau = 10^{-8} \quad \text{and} \quad \tau' = 10^{-2}.$$

The results are relatively insensitive to this choice of  $\tau$  and  $\tau'$ . An error of a factor of  $10^4$  in the estimation of  $\tau$  and  $\tau'$  produces only one order of magnitude error in  $n$  or in  $n'$  in Eqs. (22) and (23).  $\tau''$  can be estimated more critically because of the steep slope in  $\ln T_{1p}$  at the low-frequency end. The calculated curves and the measured points are shown in Fig. 3. The values of the parameters  $n$ ,  $n'$ , and  $n''$  in Eqs. (22) and (23) for these curves are shown in Table I.

It is noted that the difference between  $T_1$  and  $T_{1p}$  is very small. It is practically negligible if the spin-lattice relaxation is described by a diffusion-limited process,<sup>21</sup> Eqs. (10) and (11). The density of the paramagnetic centers can be deduced for three types of centers. The following values for the parameter were used:

$$S_i \text{ in Eq. (15)} = \frac{1}{2}; \quad a \text{ in Eq. (7)} = 4 \times 10^{-8} \text{ cm,}$$

and

$$T_2 \text{ in Eq. (7)} = 1.3 \times 10^{-3} \text{ sec.}$$

The density of the centers,  $N_\tau$ ,  $N_{\tau'}$ , and  $N_{\tau''}$  thus derived is shown in Table II. These values have no meaning beyond the order of magnitude. The relative magnitude among the values may be more significant. Nevertheless the table indicates the following facts:

TABLE II. The density of paramagnetic centers.

|     | $N_\tau$           | $N_{\tau'}$          | $N_{\tau''}$       |
|-----|--------------------|----------------------|--------------------|
| (b) | $2 \times 10^{14}$ | $0.3 \times 10^{16}$ | $1 \times 10^{17}$ |
| (c) | 3                  | 2                    | 2                  |
| (d) | 150                | 3                    | 2.5                |

(i) The white light increases  $N_T$  significantly. Lambe<sup>26</sup> observed a weak broad EPR line for this sample, when the sample was illuminated with white light. This EPR line may be associated with  $N_T$ .

(ii)  $N_T$  decreases significantly when the white light is turned off.

(iii) The red-light treatment reduces predominantly  $N_{T'}$  centers.

(iv)  $N_{T''}$  does not change appreciably with the illuminating condition. One may speculate that these centers are filled even for dark cold samples.

## B. Double Resonance in the Rotating Frame

When the sample is not illuminated,  $T_1$  and  $T_{1\rho}$  are very long, as shown above. The large value of  $T_{1\rho}$  is advantageous for cross relaxation experiments in the rotary frame,<sup>8</sup> because the weakest observable cross-relaxation rate is of the order of  $1/T_{1\rho}$ . It is not, however, practically convenient to wait a long time ( $>T_1$ ) for the spin magnetization to recover its equilibrium value in the laboratory frame after each crossing measurement in the rotary frame. In the case of CdS the illumination of the sample can be used as a convenient thermal switch between the spin system and the lattice. Thus the waiting time between the measurements can be reduced to about 30 min. Although all the switching processes in the experiment were done manually, it is easy to modify the system so that all the steps are performed automatically. Such an automatic system is almost indispensable for an extensive study of double-resonance experiments in the rotary frame.

### 1. Observation of $S^{33}$ Line

Since the natural abundance of  $S^{33}$  is only 0.74% and its nuclear resonance frequency is very low (3.266 Mc/sec at 10 kG), it is prohibitively difficult to observe the  $S^{33}$  line in solids without enrichment. Dehmelt<sup>27</sup> observed the pure quadrupole resonance of  $S^{33}$  in unenriched sulfur powder. This is the only successful observation of the S line in unenriched solids as far as the authors know.

The double-resonance technique in the rotary frame was successfully applied to observe a strong  $S^{33}$  line in the CdS sample. The rf voltage across the outside coil  $L_2$  was about 60 V, which was the maximum value available using the present setup. This value turned out to be smaller than the value needed to satisfy Hahn's optimum matching condition, Eq. (4), because the smaller  $\gamma$  value for  $S^{33}$  requires a larger value of  $H_1$ .

Nevertheless, a strong signal was observed, as shown in Fig. 4. In this figure the signal intensity of the sensor  $Cd^{113}$  nucleus was plotted after crossing in the rotary frame with  $S^{33}$  for 4 min. The signal intensity of the Cd is expressed relative to the value before the crossing. The phase of the second rf, appropriate to  $S^{33}$ , was

<sup>26</sup> J. J. Lambe (private communication).

<sup>27</sup> H. G. Dehmelt, Phys. Rev. **91**, 313 (1953).

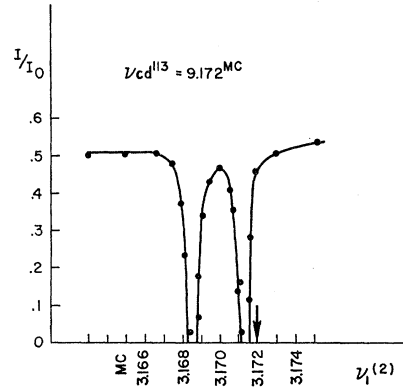


FIG. 4.  $S^{33}$  NMR line in CdS. The doublet structure is caused by the fact that the optimum matching condition for double resonance in the rotary frame, Eq. (4), is not satisfied. The vertical arrow indicates the value,  $\nu_{Cd^{113}} \times \gamma_{S^{33}} / \gamma_{Cd^{113}}$ .

flipped by  $180^\circ$  every few msec. The optimum sensitivity was obtained for a period between  $180^\circ$  phase changes of about 2 msec. Therefore, the cross relaxation time between S and Cd is this order of magnitude. It is not advantageous to reduce the value of  $H_1$  for  $Cd^{113}$ ,  $H_{11}$  to satisfy Eq. (4), or even to reduce  $H_{11}$  to zero adiabatically (adiabatic demagnetization in the rotary frame<sup>7,12</sup>), because of the sharp drop in  $T_{1\rho}$  at lower value of  $H_{11}$ .

The observed doublet line can be interpreted in terms of the small mismatching of the condition (4), as already shown by Hahn.<sup>8</sup>  $H_0$  must not necessarily be equal to exactly  $\omega_2/\gamma_2$ . A more general matching condition is to match the Larmor frequencies for both species in their effective fields,

$$[(2\pi\Delta\nu_2)^2 + (\gamma_2 H_{12})^2]^{1/2} = \gamma_1 H_{11}. \quad (24)$$

Here  $\Delta\nu_2$  is the frequency deviation of the second rf from the exact Larmor frequency. When  $|\gamma_2 H_{12}| < |\gamma_1 H_{11}|$ , Eq. (24) can be satisfied with two values of  $\Delta\nu_2$ , which give doublet lines about the Larmor frequency of the second nucleus when the second rf is swept. The intensity of the signal decreases, however, as

$$(\gamma_2 H_{12})^2 / [(2\pi\Delta\nu_2)^2 + (\gamma_2 H_{12})^2],$$

when the degree of the mismatching increases. If  $|\gamma_1 H_{11}|$  is larger than  $|\gamma_2 H_{12}|$  by a factor of, say, three or more,

$$\Delta\nu_2 \approx \pm \gamma_1 H_{11} / 2\pi. \quad (25)$$

The doublet separation can be used to measure the value of  $H_{11}$ . In the present experiment, it was found that the relation (25) was satisfied within experimental error, because there was no noticeable change in the doublet separation when  $H_{12}$  was reduced to half. The value for  $\gamma_1 H_{11} / 2\pi$  thus obtained, 1.4 kc/sec, agreed well with the value measured using the rotary saturation method.<sup>5</sup>

The center frequency of the doublet,  $3.1699 \pm 0.0002$  Mc/sec, is slightly ( $2.0 \pm 0.2$  kc/sec) lower than the value calculated from the  $Cd^{113}$  frequency, 9.1720 Mc/sec, and the ratio between  $\gamma_{Cd^{113}}$  and  $\gamma_{S^{33}}$ . This dis-



crepancy,  $7 \times 10^{-4}$ , may come from (i) chemical shift of the Cd and the S NMR frequency, and (ii) a second-order quadrupole shift of the  $(+\frac{1}{2} \leftrightarrow -\frac{1}{2})$  line of  $S^{33}$ .

Since the chemical shift of the I and Br NMR line in alkali halides<sup>28</sup> is of the order of  $1-6 \times 10^{-4}$ , the observed amount of the shift for CdS can well be due to the chemical shift of Cd. The minimum interatomic distance between Cd and S in this crystal, 2.51 Å, is less than the sum of the ionic radii 2.81 Å suggesting appreciable covalency or overlap, which could produce a sizeable chemical shift. It would be interesting to measure the chemical shift of Cd directly.

Each sulfur atom is surrounded by a tetrahedron of Cd's, which has a three-fold symmetry axis along the *c* axis. Since the Cd-S distance along the *c* axis, 2.51 Å, is slightly shorter than the other three, 2.53 Å, it is expected that there is a small electric field gradient at the position of the S nucleus. The direction of the maximum principal axis of this field-gradient tensor is along the *c* axis because the crystal structure has three-fold symmetry about this axis. A small misalignment of the *c* axis from the direction of the static field  $H_0$ , which is less than  $\pm 10^\circ$  in the present case, would reduce the center line  $(+\frac{1}{2} \leftrightarrow -\frac{1}{2})$  frequency because of the second-order quadrupole effect.<sup>29</sup> The amount of the frequency shift is<sup>30</sup>

$$\Delta\nu = (3/64)((eqQ)^2/\nu_0)(1 - \cos^2\theta)(1 - 9 \cos^2\theta), \quad (26)$$

where  $\theta$  is the angle between the maximum principal axis of the field-gradient tensor and the direction of  $H_0$ . Although no systematic study was attempted to measure the  $\theta$  dependence of  $\Delta\nu$ , it is unlikely that there is a large change in  $\Delta\nu$  when  $\theta$  is changed by about  $10^\circ$ . Therefore  $eqQ$  is estimated to be less than 1 Mc/sec.

We could not find any satellite lines  $(\pm\frac{1}{2} \leftrightarrow \pm\frac{3}{2})$  in the range  $3 \pm 1$  Mc/sec. The possible reason is either (i),  $eqQ$  is so small that the satellites are not resolved from the center line, or (ii), the satellites have been broadened below the noise level because of the imperfections of the crystal.

In any case a systematic study of the  $S^{33}$  line as a function of  $\theta$  would give a more definite value of  $eqQ$  and possibly useful information about the electronic structure of the Cd-S bond.

## 2. The NMR Line of Cd Inside the Diffusion Barrier

The NMR of the Cd nuclei near the paramagnetic centers was observed using the double-resonance technique in the rotary frame. The sensitivity of conventional NMR does not permit direct observation of these nuclei. The frequency of the first rf was tuned to the distant  $Cd^{113}$  nuclei, and the signal of these nuclei was used as a sensor of the minority nearby neighbors. The

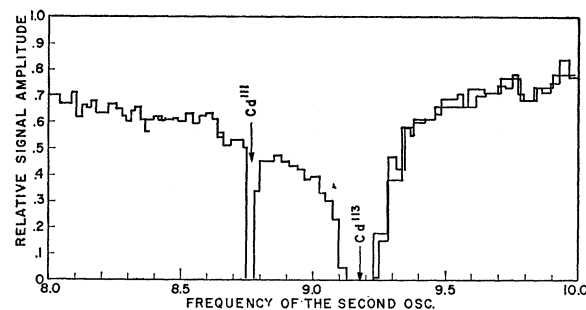


FIG. 5. NMR of the Cd nucleus in the diffusion barrier using double-resonance in the rotary frame.

matching condition (4) could be satisfied easily in this case. The frequency of the second rf was scanned about the frequency of the distant  $Cd^{113}$ . Both nuclei were brought into the rotary frame simultaneously, and the energy of the second rf field was transferred to the first spin through the crossing with the second spin system for 4 min. The  $180^\circ$  phase-modulation period was 100 msec. During this process the frequency of the second rf was swept by about 70 kc/sec. After each spin-crossing process, the remaining intensity of the first spin moment was measured by returning to the laboratory frame, as mentioned in the previous section.

The result is shown in Fig. 5. The curve indicates a widely spread tail caused by the nuclei in the diffusion barrier. The line of another isotope  $Cd^{111}$  is also observed. There seems to be a slight bump at 9.82 Mc/sec, which may be due to the nearest neighbors of some of the centers shifted by hyperfine field. The presence of at least three species of centers suggested from the analysis of the previous section may have smeared out almost all of the possible detailed structure of the tail.

## CONCLUSION

The spin-lattice relaxation time of Cd nuclei was measured both in the laboratory and the rotating frame under various optical illuminating conditions. The dependence of the relaxation time upon the illuminating condition and the magnitude of the magnetic field was interpreted in terms of spin diffusion. The results of the analysis give a rough order of magnitude of the paramagnetic center density. An experiment using double resonance in the rotary frame was reported. The NMR of the nearby nucleus about these paramagnetic centers and of  $S^{33}$  were observed.

## ACKNOWLEDGMENTS

Discussions with J. Lambe, R. Terhune, and D. K. Donald are gratefully acknowledged.

## APPENDIX A

The Hamiltonian of the spin system is

$$\mathcal{H} = \mathcal{H}_s + \mathcal{H}_a + \mathcal{H}_1 + \mathcal{H}_{SL}, \quad (A1)$$

<sup>28</sup> Yukio Yamagata, J. Phys. Soc. Japan **19**, 10 (1964).

<sup>29</sup> R. V. Pound, Phys. Rev. **79**, 123 (1950).

<sup>30</sup> For instance, A. H. Silver and P. J. Bray, J. Chem. Phys. **31**, 47 (1959).

where

$$\begin{aligned}\mathcal{H}_z &= -\gamma\hbar H_0 \sum_i I_{iz}, \\ \mathcal{H}_d &= \sum_{i>j} \gamma^2 \hbar^2 (\mathbf{I}_i \cdot \mathbf{I}_j \cdot \mathbf{r}_{ij}^{-3} - 3\mathbf{r}_{ij} \cdot \mathbf{I}_i \mathbf{r}_{ij} \cdot \mathbf{I}_j \cdot \mathbf{r}_{ij}^{-5}), \\ \mathcal{H}_1 &= -\gamma\hbar 2H_1 \cos\omega_0 t \sum_i I_{iz}, \\ \mathcal{H}_{SL} &= \text{spin-lattice relaxation term.}\end{aligned}$$

The equation of motion of a density matrix,  $\rho$  is

$$d\rho/dt = i/\hbar [\rho, \mathcal{H}_z + \mathcal{H}_d + \mathcal{H}_1 + \mathcal{H}_{SL}]. \quad (\text{A2})$$

A standard coordinate transformation into a system rotating at the Larmor frequency,  $\omega_0 = \gamma H_0$ , transforms Eq. (A2) into<sup>31,32</sup>

$$\frac{d\rho_r}{dt} = \frac{i}{\hbar} [\rho_r, \mathcal{H}_{1r} + \mathcal{H}_{dr} + \mathcal{H}_{SLr}], \quad (\text{A3})$$

where

$$\mathcal{H}_{1r} = -\gamma\hbar H_1 \sum_i I_{izr}.$$

$\mathcal{H}_{dr}$  and  $\mathcal{H}_{SLr}$  are the dipole and the spin-lattice interactions expressed in the rotating frame, respectively.

A transformation into an interaction representation in the *rotary frame*,

$$\rho_r(t) = \exp(-i/\hbar \mathcal{H}_{1r} t) \rho_r^*(t) \exp(i/\hbar \mathcal{H}_{1r} t), \quad (\text{A4})$$

gives

$$d\rho_r^*/dt = (i/\hbar) [\rho_r^*, \mathcal{H}_{dr}^* + \mathcal{H}_{SLr}^*]. \quad (\text{A5})$$

Here, since all the formalism is the same as in the laboratory frame except for the rotating frame subscript  $r$  the time dependence of the expectation value of  $I_{zr}$  can be expressed in the same form as in the laboratory laboratory frame<sup>31</sup> except for the subscript. If we only consider the part caused by the spin-lattice relaxation  $(\partial\langle I_{zr} \rangle / \partial t)_{SLr}$ ,<sup>31</sup>

$$\begin{aligned}(\partial\langle I_{zr} \rangle / \partial t)_{SLr} &= -\gamma^2 [k_{xx}{}^r(\omega_r) + k_{yy}{}^r(\omega_r)] \\ &\quad \times \{ \langle I_{zr} \rangle - I_{zr}{}^0 \}. \quad (\text{A6})\end{aligned}$$

Here

$$k_{qq}{}^r(\omega_r) = \frac{1}{2} \int_{-\infty}^{\infty} \langle H_{qr}(t) H_{qr}(t+\tau') \rangle_{\text{av}} \cos\omega_r \tau' d\tau', \quad (\text{A7})$$

$I_{zr}{}^0$  is a thermal equilibrium value of  $\langle I_{zr} \rangle$ , and

$$\mathcal{H}_{SLr}(t) = \sum_q H_{qr}(t) K_{qr}, \quad q = x, y, z. \quad (\text{A8})$$

$K_{qr}$  is the nuclear spin part of  $\mathcal{H}_{SLr}$ .

When the nucleus is relaxed by a paramagnetic electron spin,  $H_{qr}(t)$  contains electron-spin operators. But they can be considered as random time-dependent quantities. Equation (A7) can be expressed in terms of the quantities in the laboratory frame using the

<sup>31</sup> For instance, C. P. Slichter, *Principles of Magnetic Resonance* (Harper & Row, New York, 1963), p. 133f.

<sup>32</sup> A. G. Redfield, IBM J. Research Develop. 1, 19 (1957).

relations,

$$H_{yr} = H_z,$$

$$H_{xr} = H_x(t) \cos(\varphi + \omega_0 t) + H_y(t) \sin(\varphi + \omega_0 t),$$

as

$$\begin{aligned}k_{xx}{}^r(\omega_r) &= \frac{1}{4} \int_{-\infty}^{\infty} [\langle H_x(t) H_x(t+\tau') \rangle_{\text{av}} \\ &\quad + \langle H_y(t) H_y(t+\tau') \rangle_{\text{av}}] \cos\omega_0 \tau' \cos\omega_r \tau' d\tau',\end{aligned}$$

and

$$k_{yy}{}^r(\omega_r) = \frac{1}{2} \int_{-\infty}^{\infty} \langle H_z(t) H_z(t+\tau') \rangle_{\text{av}} \cos\omega_r \tau' d\tau'.$$

If we assume that the random fluctuation of  $H_q(t)$  is expressed by a correlation time  $\tau$ ,

$$\langle H_q(t) H_q(t+\tau') \rangle_{\text{av}} = \langle H_q(0)^2 \rangle_{\text{av}} e^{-|\tau'|/\tau},$$

the relaxation term in equation (A6) becomes

$$\begin{aligned}&\gamma^2 [k_{xx}{}^r(\omega_r) + k_{yy}{}^r(\omega_r)] \\ &= \frac{\gamma^2}{2} \{ \langle H_x(0)^2 \rangle_{\text{av}} + \langle H_y(0)^2 \rangle_{\text{av}} \} \frac{1}{2} \left\{ \frac{\tau}{1 + \tau^2(\omega_0 + \omega_r)^2} \right. \\ &\quad \left. + \frac{\tau}{1 + \tau^2(\omega_0 - \omega_r)^2} \right\} + \gamma^2 \langle H_z(0)^2 \rangle_{\text{av}} (\tau / (1 + \tau^2 \omega_r^2)) \\ &= \frac{\gamma^2}{2} \{ \langle H_x(0)^2 \rangle_{\text{av}} + \langle H_y(0)^2 \rangle_{\text{av}} \} (\tau / (1 + \tau^2 \omega_0^2)) \\ &\quad + \gamma^2 \langle H_z(0)^2 \rangle_{\text{av}} (\tau / (1 + \tau^2 \omega_r^2)). \quad (\text{A9})\end{aligned}$$

The corresponding relaxation term in the laboratory frame is

$$\begin{aligned}&\gamma^2 [k_{xx}(\omega_0) + k_{yy}(\omega_0)] \\ &= \{ \langle H_x(0)^2 \rangle_{\text{av}} + \langle H_y(0)^2 \rangle_{\text{av}} \} (\tau / (1 + \tau^2 \omega_0^2)). \quad (\text{A10})\end{aligned}$$

When the nucleus is relaxed by a paramagnetic electron,

$$\langle H_z(0)^2 \rangle_{\text{av}} = \frac{1}{3} S(S+1) \hbar^2 \gamma_e^2 (1 - 3 \cos^2 \theta)^2 r^{-6}, \quad (\text{A11})$$

$$\langle H_x(0)^2 \rangle_{\text{av}} = \frac{1}{3} S(S+1) \hbar^2 \gamma_e^2 (3 \cos \theta \sin \theta)^2 \cos^2 \Phi r^{-6}, \quad (\text{A12})$$

$$\langle H_y(0)^2 \rangle_{\text{av}} = \frac{1}{3} S(S+1) \hbar^2 \gamma_e^2 (3 \cos \theta \sin \theta)^2 \sin^2 \Phi r^{-6}. \quad (\text{A13})$$

In order to calculate a net-relaxation time, one must include a spin-diffusion term as well as the direct relaxation term obtained above. This relaxation term, therefore, represents the second term of the diffusion Eq. (8). After taking an angular average of Eqs. (A11), (A12), and (A13), one gets from Eq. (A9)

$$\begin{aligned}C_r &= \frac{1}{3} S(S+1) \\ &\quad \times \hbar^2 \gamma^2 \gamma_e^2 \left[ \frac{4}{3} (\tau / (1 + \omega_r^2 \tau^2)) + (\tau / (1 + \omega_0^2 \tau^2)) \right]. \quad (\text{A14})\end{aligned}$$

The corresponding value in the laboratory frame is Eq. (9). Solomon<sup>22</sup> has calculated  $C_r$  when  $\omega_r = 0$ .